

Abelian Sandpile Model on Symmetric Graphs

Natalie J. Durgin

Francis Edward Su, Advisor

David Perkinson, Reader

May, 2009

HARVEY MUDD
COLLEGE

Department of Mathematics

Copyright © 2009 Natalie J. Durgin.

The author grants Harvey Mudd College the nonexclusive right to make this work available for noncommercial, educational purposes, provided that this copyright statement appears on the reproduced materials and notice is given that the copying is by permission of the author. To disseminate otherwise or to republish requires written permission from the author.

Abstract

The abelian sandpile model, or chip-firing game, is a cellular automaton on finite directed graphs often used to describe the phenomenon of self-organized criticality. Here we present a thorough introduction to the theory of sandpiles. Additionally, we define a symmetric sandpile configuration, and show that such configurations form a subgroup of the sandpile group. Given a graph, we explore the existence of a quotient graph whose sandpile group is isomorphic to the symmetric subgroup of the original graph. These explorations are motivated by possible applications to counting the domino tilings of a $2n \times 2n$ grid.

Contents

Abstract	iii
Acknowledgments	ix
1 Introduction to the Theory of Sandpiles	1
1.1 Origins of the Model	1
1.2 Model Structure and Definitions	3
1.3 Standard Sandpile Theorems	7
1.4 Sandpile Literature	13
1.5 Alternate Approaches to Standard Theorems	14
2 Symmetric Sandpiles	19
2.1 Applications to Tiling Theorems	19
2.2 Graphs with Symmetry	21
2.3 Summary of Notation	25
2.4 The Symmetric Sandpile Subgroup	26
3 Developing a Quotient Graph	29
3.1 The Row Quotient	30
3.2 The Row Quotient Transposed	32
3.3 The Column Quotient	33
3.4 The Folded Quotient	35
4 Conclusions and Future Study	41
Bibliography	43

List of Figures

1.1	The Sandpile	2
1.2	Self-Organized Criticality	3
1.3	Directed Graph	4
1.4	A Sandpile Configuration on a Graph	6
1.5	Stabilization	8
1.6	Visualizing the Sandpile Group	11
1.7	Sandpile Group Identities	12
1.8	Big Identity	12
1.9	Small Graph	15
1.10	Visualizing the Size of the Sandpile Group	16
1.11	Alternative Proof of Uniqueness	17
2.1	Motivation for Exploring Symmetric Group Action	20
2.2	Identifying Graph Symmetry	22
2.3	Symmetric Sandpiles	23
2.4	Group Action on Vertices	24
3.1	The <i>Row Quotient Graph</i>	29
3.2	Another Row Quotient Example	32
3.3	Graph with Selfish Vertex	33
3.4	The Column Quotient Counterexample	34
3.5	The <i>Folded Quotient Graph</i>	36
3.6	Another Folded Quotient Graph Example	37

Acknowledgments

I would like to thank my advisor, Francis Su, for supporting my work on this project, for his limitless patience, for his help sorting out my confusions, and for setting an example of excellence in researching and communicating mathematics. I would also like to thank my second reader, David Perkinson, for introducing me to the problem, advising me in his area of expertise, and working with me from across several states. I would like to extend my gratitude to the entire Harvey Mudd College mathematics department for their tireless support and instruction. A special thanks goes to Claire Connelly for developing an excellent \LaTeX and thesis infrastructure and for her detailed feedback on drafts of this thesis. Finally, I would like to thank my parents for always believing in me, supporting me in all my endeavors, and encouraging me spiritually and mentally.

Chapter 1

Introduction to the Theory of Sandpiles

Imagine vacationing at the seashore as a small child. Observing a parent constructing a sand castle, we watch as they fill up a bucket with moist sand, pack it tightly, and then invert the bucket onto the ground, depositing a well-formed turret. Attempting to imitate this process, we fill up our pail with dry sand and then invert it. Lifting it up, we watch, surprised, as the dry sand cascades over its boundaries because the gradient of the pail is too steep for the dry sand to maintain such a rigid shape. We scoop more sand onto the pile to fix this problem, but instead of making the sides steeper, the added sand rolls down the sides of the pile until the avalanche stops and the pile stabilizes, assuming a conic shape with gradually sloping sides. As depicted in Figure 1.1, if we continued sprinkling sand onto the pile, we would observe that the sand pile would undergo periods of stasis with intermittent avalanches as the sides became too steep to hold their shape. These avalanches occur regularly and have different effects. How can we describe these phenomena?

1.1 Origins of the Model

In 1986 the physicists Bak, Tang, and Wiesenfeld developed a cellular automaton to describe the behavior of a sand pile. They imagined a sand pile simplified to a square grid of cells as shown in Figure 1.2. Next, a sand grain is dropped onto a random grid cell. When a cell amasses four grains of sand, it becomes unstable and the grains are redistributed to each of its adjacent grid cells. If the unstable cell is on the boundary of the grid, then

2 Introduction to the Theory of Sandpiles

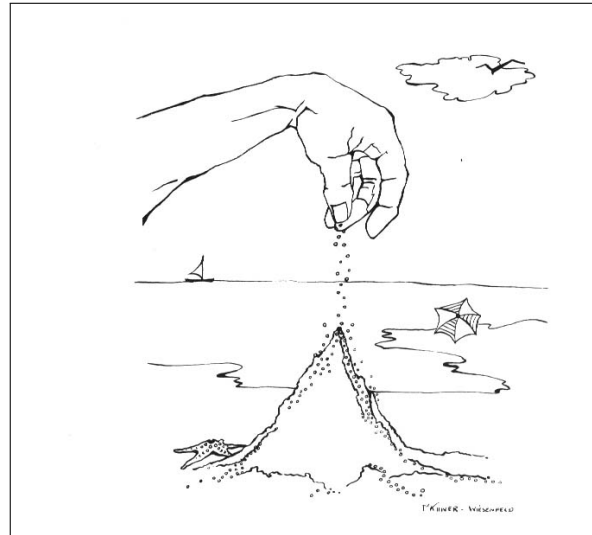


Figure 1.1: Sand piles exhibit static periods with intermittent sand slides, (Bak, 1996).

three grains of sand will be transferred to neighboring cells, and one grain will fall off the edge and disappear. If the cell is on the corner of the grid, then two grains will be transferred to neighboring cells and two will fall off the edge and disappear. The number of sand grains on a particular cell may be thought of as the “local slope” of the sandpile. As the sand percolates over the grid in this fashion, adjacent cells may accumulate four grains of sand and become unstable causing an “avalanche.” What governs the frequency of these avalanches?

Many physicists are very interested in the frequency, size, and duration of these avalanches. It has been demonstrated that the distribution of avalanches has a fractal structure, and thus has nontrivial correlations with power-law decay. Many phenomena in nature exhibit this fractal structure. In Dhar (1999), several examples of this power-law decay are explained. For example, the author cites spatial fractal behavior, such as the height profile of mountain ranges or the drainage area of a river as we travel downstream. The author also cites nonspatial examples of fractal behavior, such as the Gutenberg-Richter law, which says that the frequency of an earthquake of total energy E is found to vary as E^{-z} , where z is a number close to 2, for many decades of the energy range. Another compelling example comes from fluid turbulence, where the fractal behavior is

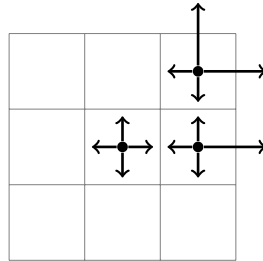


Figure 1.2: The Bak, Tang and Wiesenfeld model of self-organized criticality.

observed in the way mean-squared velocity difference scales with distance, or in the spatial fractal structure of regions of high dissipation.

Systems that exhibit this significant correlation with power-law decay are said to have critical correlations. For equilibrium systems, such as a block of ice, these critical correlations to power-law decay are replaced by a critical phase transition. Such critical points can only be achieved by adjusting some physical parameter such as the temperature of the system. The behavior of a nonequilibrium system is independent of control parameters and will achieve its critical state independent of any control parameter. Such a system is said to exhibit *self-organized criticality*. A system that exhibits self-organized criticality will have a constant “input” (steady addition of sand grains), and a series of events or “avalanches” as “output” (sand avalanches). The “output” follows a power-law (fractal) frequency-size distribution. Self-organized criticality has been used to describe systems such as forest fires, earthquakes, and stock-market fluctuations (Bak, 1996). Understanding such systems, then, should lead to numerous physical applications.

1.2 Model Structure and Definitions

The sandpile model was first generalized and developed by Dhar (1990). To understand his generalization, we recall some basic graph theory. A *directed graph* Γ is a finite, nonempty set V (the vertex set) together with a disjoint set E (the edge set), possibly empty, that contains ordered pairs of distinct elements of V . An element of V is called a *vertex* and an element of E is called an *edge*. Altogether, we denote the graph $\Gamma(V, E)$. Let $v_1, v_2 \in V$.

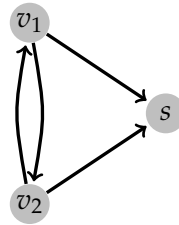


Figure 1.3: This directed graph has a global sink.

If there exists an edge $(v_1, v_2) \in E$, we say the vertices v_1 and v_2 are *adjacent*. In Figure 1.3, we find an example graph $\Gamma(V, E)$. Here the graph has vertex set $V = \{v_1, v_2, s\}$ and the edge set

$$E = \{(v_1, v_2), (v_1, s), (v_2, v_1), (v_2, s)\}.$$

This graph is called a *multigraph* because we allow more than one edge (but a finite number) to connect a pair of vertices. We say a graph has *self-loops* if there are edges connecting a vertex to itself.

Recall that the Bak-Tang-Weisenfeld (BTW) sandpile model was defined on square grids with cells that randomly received sand grains. These cells had a maximum capacity of 3 sand grains; once this capacity was exceeded, the sand would topple into adjacent cells or fall off the edge of the grid. These square grids are a type of graph, with the cells as the vertices and edges connecting adjacent cells and allowing sand grains to pass from one cell to a neighboring cell.

In order to generalize this concept, Dhar decided to consider a finite directed graph $\Gamma = (V, E, s)$ with multiple edges and self-loops allowed. The graph has a designated vertex s called the *sink*. We keep Figure 1.3 in mind as we define the following terms. Each non-sink vertex of Γ has a number of edges directed away from it. This number is called the out-degree of vertex v and is denoted d_v . In our example, $d_{v_1} = 2$. If a sink s has a directed path going into it from every other vertex, then s is called a *global sink*. In our example graph, s is global because both v_1 and v_2 have an edge directed into it. Note that if a global sink exists it must be unique. Suppose both s and s' are global sinks, then s must have a directed edge to s' , but this contradicts the definition of a sink.

We would like to have an algebraic structure for associating sand grains to the vertices of the graph. Informally, we might think of a sandpile as a nonnegative integer weighting on the n vertices of a graph, taking the form

of a vector $\sigma \in \mathbb{Z}^n$.

More formally, let X be any finite set. Fix an ordering on the elements of X : x_1, x_2, \dots, x_n . Then consider the standard basis for \mathbb{Z}^n , $\{e_1, e_2, \dots, e_n\}$. Associate to each element of X a standard basis element in the natural way, $x_i := e_i$. Recall that a *free abelian group* is an abelian group in which every group element can be written uniquely as a finite linear combination of basis elements. Define a free abelian group on X in the following way:

$$\mathbb{Z}X = \left\{ \sum_{x \in X} c_x x : c_x \in \mathbb{Z} \text{ for all } x \in X \right\}$$

In order to formally define a sandpile, we will also need to define an object that restricts our “scalars” to the nonnegative integers.

$$\begin{aligned} \mathbb{N}X &= \{c \in \mathbb{Z}X : c \geq 0\} \\ &= \left\{ \sum_{x \in X} c_x x : c_x \geq 0 \text{ for all } x \in X \right\}. \end{aligned}$$

Definition 1.1: Given a graph $\Gamma(V, E, s)$, let \tilde{V} denote the non-sink vertices. A *sandpile configuration* on Γ is an element of $\mathbb{N}\tilde{V}$.

To capture the structure of the graph in matrix form, we define Δ to be the *graph Laplacian*. To define this matrix we first consider the adjacency matrix A . Let $V = \{v_1, v_2, \dots, v_n\}$, then the entries of A are given by $A_{ij} = w(v_i, v_j)$, where w denotes the edge weight, that is the number of directed edges from vertex v_i to vertex v_j . We must also consider the diagonal matrix D , whose diagonal entries are equal to the out-degree of each vertex. The graph Laplacian is an $n \times n$ matrix given by $\Delta = D - A$.

Example 1.1: Referencing the graph in Figure 1.3 we proceed to compute the Laplacian matrix. We note that the out-degree of both vertices is 2, and the has no out-degree. This gives us the diagonal entries of D . Next we compute the adjacency matrix and subtract:

$$\Delta = D - A = \begin{pmatrix} 2 & 0 & 0 \\ 0 & 2 & 0 \\ 0 & 0 & 0 \end{pmatrix} - \begin{pmatrix} 0 & 1 & 1 \\ 1 & 0 & 1 \\ 0 & 0 & 0 \end{pmatrix} = \begin{pmatrix} 2 & -1 & -1 \\ -1 & 2 & -1 \\ 0 & 0 & 0 \end{pmatrix}.$$

Note that the rows of the Laplacian matrix sum to zero. In the sandpile context, this tells us that the amount of sand that topples off an unstable vertex is the same amount gained by its adjacent vertices. We will discuss this further in the next section.

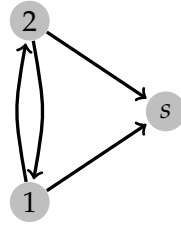


Figure 1.4: A sandpile configuration can be thought of as a nonnegative, integer weighting on the vertices.

The *reduced Laplacian* of Γ is the Laplacian matrix we obtain by deleting row and column corresponding to the sink, e.g.

$$\tilde{\Delta} = \begin{pmatrix} 2 & -1 \\ -1 & 2 \end{pmatrix}.$$

Notice that the original Laplacian can always be recovered from the reduced Laplacian by adding a row of zeros to the bottom of $\tilde{\Delta}$, and adding a new column with values that ensure all rows sum to zero. The reduced Laplacian will be an important tool in describing sand avalanches. Now that we have built a generalized structural framework for our model, we can begin to drop on sand.

An example of a sandpile on the graph in Figure 1.4 would be $\sigma = (2, 1)$, where $\sigma(v_1) = 2$ and $\sigma(v_2) = 1$. We say a configuration σ is *stable* at vertex v if $\sigma(v) < d_v$, that is, if the number of sand grains on v is less than the out-degree of the vertex. A configuration σ is *unstable* at a vertex v if $\sigma(v) \geq d_v$. If the number of grains of sand on a vertex equals or exceeds the out-degree of the vertex, then the sandpile *topples* sending one grain of sand each of its adjacent vertices. The new sandpile obtained after an unstable vertex topples is called a *successor* of σ and is denoted σ' .

Returning to the reduced Laplacian we defined earlier, we find a handy algebraic method to describe the stabilization of sandpiles. If $\sigma(v) > d_v$ then the toppling of sand on v is equivalent to subtracting the corresponding row of the reduced Laplacian from σ . In Figure 1.5, we show a toppling sequence for the sandpile $\sigma = (2, 1)$. In the first frame, we note that v_1 is unstable because $\sigma(v_1) \geq d_{v_1} = 2$.

To capture that the sand on vertex v_1 has toppled, we subtract the corresponding row of the reduced Laplacian, $(2, -1)$, from the sandpile configuration $\sigma = (2, 1)$. This gives us a new sandpile configuration $(0, 2)$. Now,

however, vertex v_2 is unstable as shown in the second frame of Figure 1.5. We subtract the row of the reduced Laplacian corresponding to vertex v_2 from the new sandpile to obtain the stable sandpile: $(0, 2) - (-1, 2) = (1, 0)$. This sandpile is called the *stabilization* of σ and we denote it σ° .

Alternatively, for a graph with n vertices, we can think of sandpiles as points in affine n -space, \mathbb{A}^n . Adding sand to a particular vertex then could be thought of as an *affine transformation*.

Definition 1.2: An *affine transformation* is a map between affine spaces and consists of a linear transformation, followed by a translation: $x \mapsto Ax + b$.

The way we have defined our toppling rules in this popular version of the model, adding sand to a graph is just a translation so $A = I$. Also, recall that we have defined a sandpile only over the positive integers so that we must always have $\sigma = Ix + b \geq 0$. Consider Figure 1.5. On the right side of each frame, we translate the sandpile via the rows of the reduced Laplacian until it is in the stable region. One might conceive of an application of this model that would require the notion of “negative” sand on a particular vertex, or toppling rules that would include a linear transformation.

Considering this process, we might be concerned that the order in which the sand grains on the vertices topple might change the long-term behavior of the system. However, the toppling order turns out to be completely inconsequential. In the following chapter we provide some standard proofs adapted from Holroyd et al. (2008) for the general existence and uniqueness of σ° independent of toppling order.

1.3 Standard Sandpile Theorems

Theorem 1.1 (Uniqueness of stabilization, independent of toppling order):

Let Γ be a finite directed graph, and let $\{\sigma_i\} = \sigma_0, \sigma_1, \dots, \sigma_n$ be a sequence of sandpile configurations on Γ , each of which is the successor of the one before it. Let $\{\sigma'_i\} = \sigma'_0, \sigma'_1, \dots, \sigma'_m$ be another such sequence with the initial states being equivalent, $\sigma'_0 = \sigma_0$. We can conclude the following:

1. Without loss of generality, if σ_n is stable, then $m \leq n$, and moreover, no vertex's sand topples more times in $\{\sigma'_i\}$ than in $\{\sigma_i\}$.
2. If σ_n and σ_m are both stable, then $m = n$, $\sigma_n = \sigma'_m$, and each vertex's sand topples the same number of times in both histories.

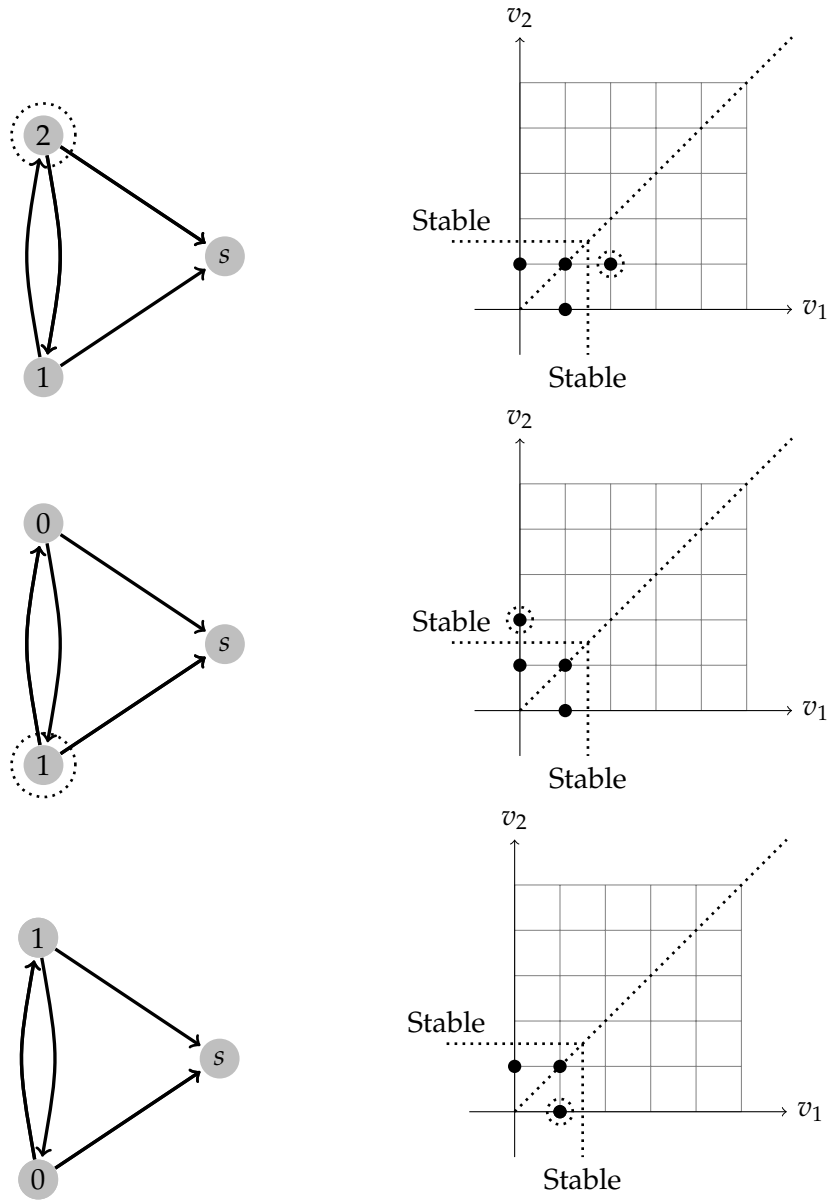


Figure 1.5: Stabilization sequence for an example graph. On the right, we trace the sandpile in the affine plane as rows of the reduced Laplacian are subtracted.

Proof. Note that the second statement follows immediately from the first. If the first statement fails, consider the counterexample with $m + n$ minimal. Let v_i be the vertex whose sand topples when σ_{i-1} becomes σ_i , and v'_i be the vertex whose sand topples when σ'_{i-1} becomes σ'_i . The sand on vertex v'_1 must topple at some stage in the sequence of configurations $\{\sigma_i\}$, since σ_n is stable. Suppose that this toppling occurs at the i th stage in the sequence so that $v_i = v'_1$. Then there exists a toppling sequence, $v_i, v_1, v_2, \dots, v_{i+1}, \dots, v_n$ that turns σ_0 into σ_n with the same number of topplings at each site as the unpermuted sequence. Thus the toppling sequences $v_1, \dots, v_{i-1}, v_{i+1}, \dots, v_n$ and v'_2, v'_3, \dots, v'_m constitute a smaller counterexample to the first statement (with initial configuration σ'_1), contradicting minimality. \square

With this theorem it is clear that if a stabilization exists for σ then it will be unique. We turn to the following theorem for existence.

Theorem 1.2: *On a directed graph with a global sink, through a sequence of topplings every configuration σ stabilizes to σ^0 .*

Proof. Suppose σ is a configuration with N grains of sand, i.e. $\sum_{i=1}^n \sigma(v_i) = N$, and $v \in \tilde{V}$. Let v_0, v_1, \dots, v_m be a directed path from $v_0 = v$ to $v_m = s$. Then v_{m-1} can fire at most N times, v_{m-2} can fire at most $d_{v_{m-1}} N$ times etc. Thus, $v = v_0$ can fire at most $d_{v_1} \dots d_{v_{m-1}} N$ times. Thus, each vertex can fire at most a finite number of times. \square

Note that this is not true if the graph has no sink. In this case, the sum of the sand over all the vertices is invariant. Choose a configuration σ such that $\sum_{i=1}^n \sigma(v_i) > \sum_{i=1}^n d_{v_i}$; such a configuration exists because \mathbb{N} is infinite and d_{v_i} is finite for all i . Then there will always be at least one vertex with the number sand grains greater than its out-degree, by the pigeon hole principle. Thus the configuration will never stabilize.

Now that we have defined the notion of toppling and stabilization, we would like to have a way to add more sand to our graph. To do this we define a special addition operator as follows:

Definition 1.3: Let σ be a stable configuration, and define the *sand addition operator*, \mathcal{S}_v , such that the stable configuration $\mathcal{S}_v \sigma$ is the configuration realized after adding a sand grain to vertex v and then stabilizing. That is, $\mathcal{S}_v \sigma = (\sigma + 1_v)^\circ$.

Theorem 1.3 (Abelian Property): *On a directed graph with a global sink, the sand addition operators commute.*

Proof. Let σ be a sandpile configuration and v_1 and v_2 be vertices. Note that the unstable vertices of $\sigma + 1_{v_1}$ form a subset of the unstable vertices of the configuration $\sigma' = \sigma + 1_{v_1} + 1_{v_2}$. So if we stabilize $(\sigma + 1_{v_1})$ we obtain $\sigma' = \mathcal{S}_{v_1}\sigma + 1_{v_2}$. Stabilizing once more we obtain $(\sigma')^\circ = \mathcal{S}_{v_2}\mathcal{S}_{v_1}\sigma$, the stabilization of σ' . Without loss of generality, we might have replaced vertex v_2 for vertex v_1 in the above argument obtaining $(\sigma')^\circ = \mathcal{S}_{v_1}\mathcal{S}_{v_2}\sigma$. Thus, $\mathcal{S}_{v_2}\mathcal{S}_{v_1}\sigma = \mathcal{S}_{v_1}\mathcal{S}_{v_2}\sigma$, by uniqueness of stabilization. Notice that we use the assumption of the existence of a global sink in order to ensure that every configuration stabilizes. \square

With an operator and the set of sandpile configurations, we are motivated to define a group structure.

Definition 1.4: The *sandpile group* for the graph Γ is given by

$$S(\Gamma) = \mathbb{Z}\tilde{V} / \text{Row}(\tilde{\Delta}(\Gamma)),$$

that is, the quotient group obtained after modding out by the integer row span, or image, of the reduced Laplacian of Γ .

For graphs with only two vertices, we can visualize this group as lattice points in the affine plane as shown in Figure 1.6. Choosing an arbitrary lattice point, we proceed to translate the sandpile by subtracting rows of the reduced Laplacian until we reach a sandpile in the stable region. Note that in Figure 1.6 each lattice point is associated to a distinguishing shape: a circle, square, or diamond. If we begin at a sandpile with a particular shape and stabilize, we find that the shape associated to the stable sandpile matches the shape with which we started. The shapes denote the equivalence classes of the group.

Throughout the process of adding sand, toppling and stabilizing, the sandpile configuration is constantly changing. There are some configurations that can never occur except as an initial state of the sandpile. These configurations are called *transient*. For example consider the zero configuration on the 3×3 grid graph. Once sand has been added to a cell, the graph will never again be empty. Suppose we dropped some sand on the cell at the center of the grid. If we keep adding sand to try and move the other grain off the grid, the sand grains on that center cell will topple once there are more than four grains, sending sand to the neighboring cells in the graph. As more sand is added, some will fall off the edge, but there will always be sand remaining on the graph. This suggests the question: what are configurations we can get to from any other configuration in the graph?

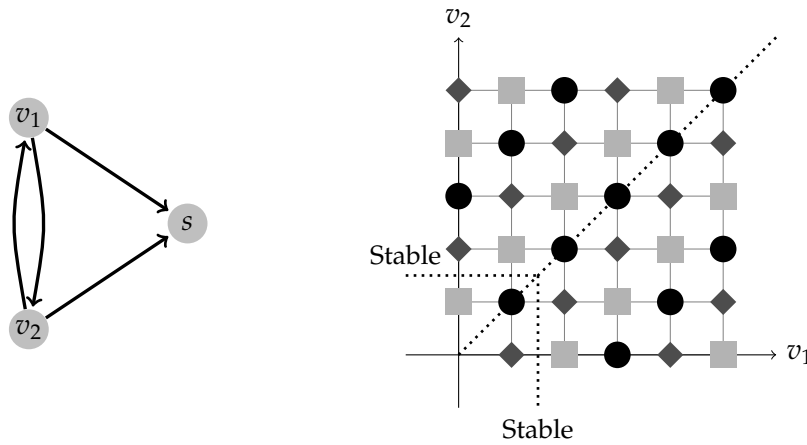


Figure 1.6: The rows of the reduced Laplacian partition the sandpiles into equivalence classes, delineated by the shapes.

A *recurrent* sandpile configuration is a stable configuration that can be obtained from any other configuration via a sequence of sand additions and topplings. The *maximum stable configuration* σ_{\max} is given by $\sigma_{\max}(v) = d_v - 1$, that is, every vertex has the most sand it can hold without toppling. The maximum stable configuration is a clear example of a recurrent configuration. It can also be shown that a configuration σ is recurrent if and only if there exists a configuration τ such that $\sigma = (\tau + \sigma_{\max})^\circ$.

As it is proved in Holroyd et al. (2008), each equivalence class of $S(\Gamma)$ contains a unique recurrent sandpile configuration and so we redefine $S(\Gamma)$ to be the group of recurrent elements of Γ . Because this is a group, we might inquire after the identity sandpile. The identity sandpile, $e \in S(\Gamma)$ can be computed as follows: $e = (2\sigma_{\max} - (2\sigma_{\max})^\circ)^\circ$.

Considering $n \times n$ graphs, the identity sandpile emerges as an interesting object of study. Figure 1.7 lists some of the identity sandpiles for small square grid graphs. Figure 1.8 is the identity sandpile for the 57×57 grid. Notice the presence of a large square in the center of the grid, which has less sand than its surrounding cells. Such a square exists in the identity sandpile for many very high values of n . This might suggest physically, that somehow the sandpile is more stable towards the center. The existence of this square in the center of the $n \times n$ grid remains an open question (Holroyd et al., 2008).

How large is this group? Consider that the order of $S(\Gamma)$ is equal to the index of the lattice $\text{Row}(\tilde{\Delta}(\Gamma))$ in $\mathbb{Z}\tilde{V}$ by definition. Consider also that

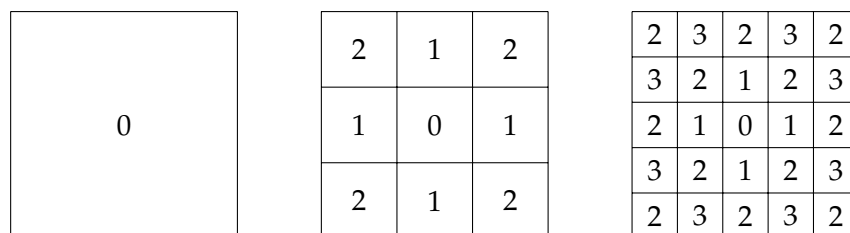


Figure 1.7: Identity Sandpiles for the 2×2 grid, 3×3 grid, and 5×5 . The integer indicates the height of the sand in each cell.

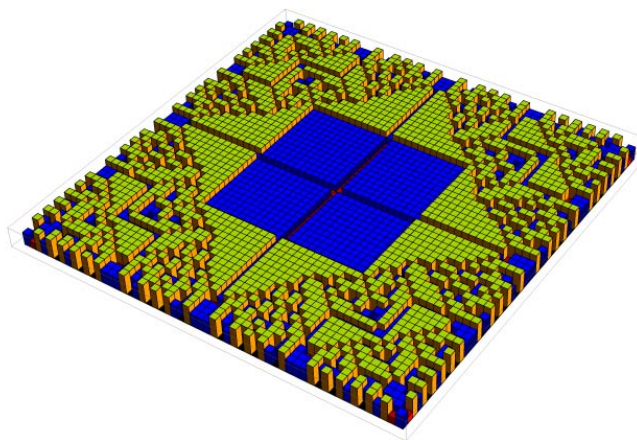


Figure 1.8: Identity sandpile for the 57×57 grid. Colors: red = 1, blue = 2, yellow = 3. Generated in Mathematica

the volume of a parallelepiped is given by the determinant of the matrix formed from its edge vectors. Since the order of $S(\Gamma)$ is the volume of the parallelepiped formed by the rows of the reduced Laplacian, the order of $S(\Gamma)$ is given by $\det(\tilde{\Delta})$.

1.4 Sandpile Literature

Here we transition from a thorough treatment of definitions and theorems to highlighting some results in the literature related to the abelian sandpile model. Many of these results require a specialized knowledge of the field, and we will not provide an in-depth discussion in this report, but include them for completeness.

1.4.1 The BTW Results

The abelian sandpile model has its roots in statistical physics and was developed as a model of self-organized criticality. As discussed earlier Bak et al. (1987) were the first to explore the physical implications of self-organized criticality and they conceived a sandpile model to describe it. Many possible applications of this model, including earthquakes, solar flares, punctuated equilibria, dinosaur extinction, brain models, traffic jams, and the economy are discussed in Bak (1996).

1.4.2 Areas of Mathematics Spanned

The sandpile model was first studied in depth and generalized by Dhar (1990, 1998, 1999), who coined the name abelian sandpile model (ASM). In his later papers he surveys known results about the model, in particular he provides all the critical exponents characterizing the distribution of avalanche-sizes in all dimensions. He introduces a relationship between the ASM and the Potts model, which models interacting spins on a crystalline lattice. He discusses a generalization of the ASM to networks of communicating reactive processors. In particular he develops sandpile models with stochastic toppling rules.

How can we tell whether or not a configuration is transient or recurrent? Dhar (2006) presents a test called the *burning algorithm*. He shows that a configuration with two adjacent vertices having a sand height of 1 must be transient. Extending this, he defines the notion of a *forbidden sub-configuration*, a set of connected vertices with particular height properties

that will render the configuration transient. Given a configuration, at first all the sites are considered unburnt. Then, burn each site (remove its sand) whose height is larger than the number of its unburnt neighbors. This process is repeated recursively, until no further sites can be burnt. Then, if all the sites have been burnt, the original configuration was recurrent, whereas if some sites remain unburnt, then the original configuration was transient, and the remaining sites form a forbidden subconfiguration.

From a discrete mathematics perspective, Merino (2005) introduces an important relation between the chip-firing game and the Tutte polynomial. This polynomial is the property of a matroid, an “independence structure” that generalizes the notion of vector space linear independence. The Tutte polynomial can be thought of as a normalized generalization of the chromatic polynomial of a graph. Here, Merino surveys the connections between chip firing and the Tutte polynomial, group theory, greedoids with repetition and matroids. He also explores relationship between the physicists’ abelian sandpile model and the Potts model.

For additional fascinating combinatorial results, Kenyon et al. (2000) explores Temperley’s bijection between spanning trees of the square grid and perfect matchings (dimer coverings) of the square grid. The authors extend this result to general planar graphs, both directed and undirected, with positively weighted edges. These weighted edges induce a weighting on the set of spanning trees. They explore two particular cases of this bijection. They define a cylinder event for random spanning trees of directed, weighted, planar graphs. Their main theorem allows them to compute the measure of all such events. They also introduce Wilson’s algorithm for quickly generating random samples of perfect matchings.

Given a sandpile group, what are the orders of its elements? That is, how many times must we add the pile to itself and stabilize before we arrive at the identity sandpile? This question was explored in Morar and Perkinson (2007). Considering the $2 \times n$ grid, the authors computed the order of the element having two grains of sand at each vertex.

1.5 Alternate Approaches to Standard Theorems

The proofs included in Section 1.3 are largely algebraic in nature. If we consider sandpiles as points in affine space, and toppling and sand addition as affine transformations, then we might be able to create geometric proofs of the same theorems. Here we present some possible approaches and proof sketches for small graphs with only two vertices. Such cases are easier to

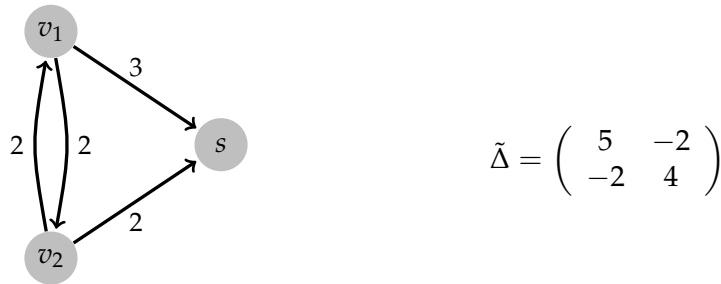


Figure 1.9: For a graph with two vertices, it is easy to visualize the size of its sandpile group.

visualize because their associated sandpiles exist in the affine plane.

For example, given a graph with only two vertices, it is very easy to visualize why the size of its sandpile group is equal to the determinant of its associated reduced Laplacian. Suppose we have the graph in Figure 1.9. Recall that as we have defined a stable sandpile, each vertex v can have any amount of sand s satisfying the condition that $0 \leq s < d_v$. Being as generous as possible then for the graph in Figure 1.9, vertex v_1 might have 0, 1, 2, 3 or 4 grains of sand, and vertex v_2 might have 0, 1, 2 or 3 grains of sand. Combinatorially, the number of possible ordered pairs (i.e. the number of stable configurations) will be 5×4 , or the product of the out-degrees of the vertices.

Plotting all possible stable configurations in the affine plane, we obtain region in Figure 1.10. Some of these configurations will not be recurrent. Experimenting, we choose several sandpiles outside of the stable region and then stabilize them by subtracting off rows of the reduced Laplacian, until we are able to translate them into the stable region. No matter how far out on the lattice we begin, following the rules of stabilization, we will never reach the sandpiles delineated by the grey squares.

These configurations are not recurrent! Also note, that for this example, the off-diagonals of the reduced Laplacian, $(2, 2)$ give the exact dimensions of the square of transient configurations. The stable, recurrent configurations that make up the sandpile group can be counted exactly by computing the determinate of the reduced Laplacian: $(5 \times 4) - (2 \times 2)$.

Question 1.1: Do these geometric properties of the sandpile group found in many small examples have any analogue for the sandpile groups of larger graphs?

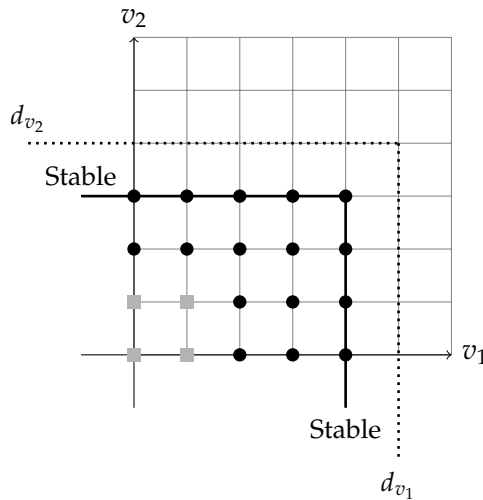


Figure 1.10: The stable sandpiles are marked with a shape. The black circles are both stable and recurrent. The squares are stable but transient. Note that the number of black dots is exactly given by the determinate of the reduced Laplacian: $(5 \times 4) - (2 \times 2)$.

If there were such geometric analogues for graphs with greater than 2 vertices, this approach might yield very intuitive proofs of many of the standard sandpile theorems.

As another example, we might recast the question whether or not sandpile stabilization is unique as the solution to a system of linear inequalities. Recall the 2-dimensional example 1.3 where,

$$\tilde{\Delta} = \begin{bmatrix} 2 & -1 \\ -1 & 2 \end{bmatrix}$$

Let $c = [c_1, c_2]$ be a column vector containing the coefficients of the columns of the reduced Laplacian that stabilize a sandpile σ . Also, let d denote the vector of out-degrees of the vertices, i.e. the vector containing the diagonal entries of the reduced Laplacian. Then consider the systems:

$$\begin{aligned} \sigma - \tilde{\Delta}^T c &\leq d - 1 \\ \sigma - \tilde{\Delta}^T c &\geq 0. \end{aligned}$$

The first equation says that we must subtract off some linear combination of the rows of the reduced Laplacian until amount of sand falls below

the out-degree of the vertex, d . This means that the number of sand grains left on vertex, v_i must be less than or equal to the out-degree of the vertex. The second equation says that the final result must not be negative. In this example, these inequalities explicitly become the two systems of inequalities:

$$\ell_1 := \sigma_1 - 2c_1 + c_2 \leq 1$$

$$\ell_2 := \sigma_2 + c_1 - 2c_2 \leq 1$$

$$\ell_3 := \sigma_2 - 2c_1 + c_2 \geq 0$$

$$\ell_4 := \sigma_2 + c_1 - 2c_2 \geq 0$$

Graphing the parallelogram that surrounds possible solutions, the stabilization of each sandpile does indeed lie in each of the shapes. Consider the graphs of these parallel lines with different y -intercepts. We overlay an integer lattice on the plane as shown in Figure 1.11

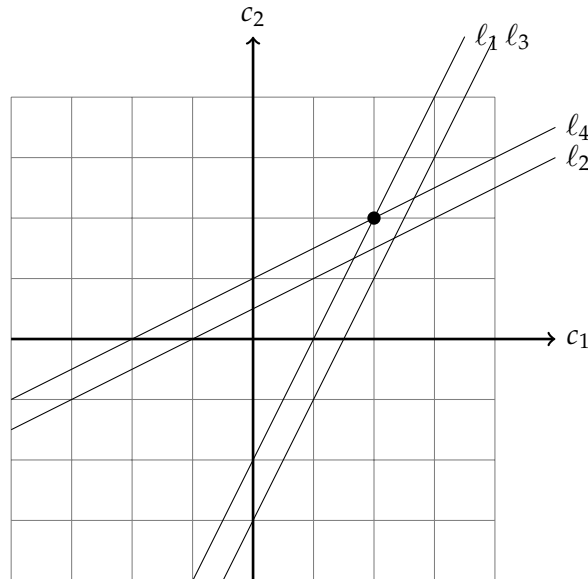


Figure 1.11: The parallelogram represents the possible coefficients for the rows of the reduced Laplacian that might yield an allowable stable configuration

Question 1.2: Might the stabilization of a sandpile σ on a graph with reduced Laplacian $\tilde{\Delta}$ be given by some special (possibly unique) point in the parallelogram of its coefficient lines?

We can easily compute the volume of the parallelogram for the 2-vertex case using Cramer's Rule,

$$\frac{\det(D - I)}{\det(\tilde{\Delta})},$$

where D is the matrix with the out-degree of each vertex along the diagonal. Based on numerous examples, it seems to be true that for the 2-vertex case this volume must be less than 1. A likely answer to Question 1.2 might show how the volume of the parallelogram restricts lattice points, in fact there can be at most one under the right conditions.

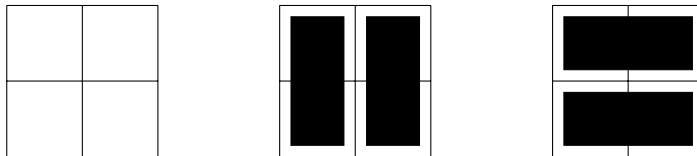
This approach certainly has some flaws as it has been described. One obvious one is that the lower bound on the stabilization is not necessarily zero. In fact it will be a *burning script* as discussed in Speer (1993). This is a configuration that conceptually gives a lower bound for the amount of sand that can be in a recurrent configuration for a given graph. This means that, for some graphs, the linear system of inequalities will yield a parallelogram that surrounds multiple lattice points. Additional conditions may be required to prove uniqueness.

Chapter 2

Symmetric Sandpiles

2.1 Applications to Tiling Theorems

Consider the problem of tiling a square grid with sides of even length using only dominos. How many domino tilings of such a $2n \times 2n$ grid exist? Consider the case where $n = 1$:



Here, there are two possible domino tilings of this grid. In general it has been shown that the number of domino tilings is $2^n a_n^2$ for some odd integer a_n . A combinatorial version of the proof for this theorem can be found in Pachter (1997). The first seven values of a_n are as follows:

a_1	a_2	a_3	a_4	a_5	a_6	a_7
1	3	29	901	89893	28793575	29607089625

The *matrix-tree theorem*, a classic result due to Tutte, gives us a special corollary: the number of spanning trees of the graph Γ is equal to the size of the sandpile group $S(\Gamma)$. It has also been shown in Kenyon, Propp, and Wilson that the number of spanning trees of a graph is in one-to-one correspondence with the domino tilings of a related graph. This motivates us to find a relationship between the sandpile group and the domino tilings of a graph.

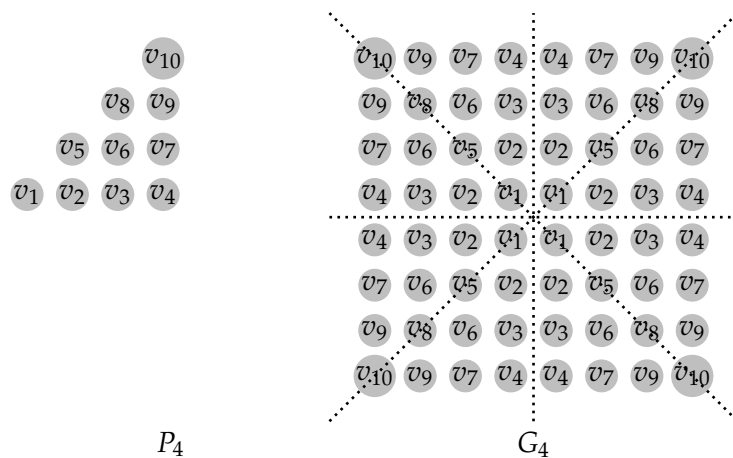


Figure 2.1: The subgraph P_4 is invariant under the dihedral group, D_4 .

We say that an $n \times m$ grid graph has *wired boundary* if it is an undirected graph and each corner vertex has an edge of weight 2 going to the sink, and all other vertices on the boundary of the grid have an edge of weight 1 to the sink. Such boundary conditions give all non-sink vertices degree 4, (Holroyd et al., 2008). Specifically, let us consider a relationship between the domino tilings of a $2n \times 2n$ grid graph with wired boundary and the size of its associated sandpile group $S(\Gamma_{2n \times 2n})$.

Such a relationship has been explored in Perkinson (2008a). Given a group $(G, +)$, recall that we define the *order* of a group element, $g \in G$, to be the least number of times we must add g to itself to obtain the identity, that is to say that the order of g is the least positive integer m such that $mg = g + \dots + g = I$. If no such integer m exists then we say that g has *infinite order*. Consider the sandpile group of a $2n \times 2n$ grid graph, $S(\Gamma_{2n \times 2n})$. Let $g_n \in S(\Gamma_{2n \times 2n})$ be the element with 2 grains of sand on every vertex. It has been shown that the order of g_n divides a_n , the number associated with the domino tilings of $\Gamma_{2n \times 2n}$.

The proof of the theorem in Perkinson (2008a) requires the construction of a subgraph of $\Gamma_{2n \times 2n}$, denoted P_n for “Pachter”, that respects the dihedral symmetry of the grid graph in the following way. Let $G_n := \Gamma_{2n \times 2n}$ for simplicity. Suppose $n = 4$ and consider Figure 2.1. Here we have a small triangular graph that we flip around the dihedral symmetries depicted by the dotted lines to obtain the large grid graph G_4 . In the following sections we will generalize the notion of a graph that captures the behavior

of a larger graph under a symmetry group action. This might allow the extension of the domino tiling theorem to other types of graphs.

2.2 Graphs with Symmetry

Consider the symmetric graph in Figure 2.2. Note how the vertices along the axis of symmetry play an equivalent role in the dynamics of the model. That is, if we place equal amounts of sand on both vertices, they will always have equal amounts of sand on them after toppling because their structure and instability conditions are the same. If we were to flip the graph about the axis of symmetry, we would obtain an identical graph.

A *group action* on a graph $\Gamma(V, E, s)$ partitions the vertex set V into equivalence classes called *orbits*. More formally, we define the action the group G on Γ to be the mapping

$$\begin{aligned} G \times V &\rightarrow V \\ (g, v) &\mapsto gv, \end{aligned}$$

That satisfies the following properties:

- (1) if e is the identity of G , then $ev = v$ for all $v \in V$;
- (2) $g(hv) = (gh)v$ for all $g, h \in G$ and $v \in V$;
- (3) if $(v, w) \in E$, the edge set, then $(gv, gw) \in E$ and both edges have the same weight.

Definition 2.1: For each $v \in V$, the *orbit* of v under G is

$$Gv = \{gv : g \in G\}.$$

Let $V^G = \{Gv : v \in V\}$ denote the set of orbits of the vertices of Γ under G .

Recall that we defined a sandpile configuration σ to be an element of the free abelian group $\mathbb{Z}\tilde{V}$, or more loosely to be a nonnegative integer weighting on the non-sink vertices of the graph. It is natural to surmise that the action of the group G on the vertices of the graph induces an action on the sandpile group, $S(\Gamma)$, and its associated algebraic objects. This is because, in some sense, the vertex set under the group action, V^G , becomes the set of orbits of the vertices of Γ under G .



Figure 2.2: The dotted line denotes an axis about which this directed graph is symmetric.

Definition 2.2: Consider the sandpile configurations $\sigma \in S(\Gamma)$. We call σ *symmetric* if $g\sigma = \sigma$ for all $g \in G$. Alternatively, we might consider symmetric configurations to assign equal weights to the vertices of a given equivalence class.

Given the properties of a group action listed above, it is important to note the following implications:

1. If $gv = gw$ for some $g \in G$, and $v, w \in V$, then $v = w$. (Multiplying by g^{-1} we obtain:

$$\begin{aligned} g^{-1}gv &= g^{-1}gw, \\ (g^{-1}g)v &= (g^{-1}g)w \text{ by (2)} \\ (e)v &= (e)w \\ (e)v &= (e)w \text{ by (1).} \end{aligned}$$

2. For all $g \in G$, we have $gs = s$, that is, the sink is necessarily a fixed point of Γ . This follows from (3).
3. The maximal stable configuration, σ_{\max} , is symmetric. (The degrees of the vertices are preserved under the group action by (3).)

To better understand the symmetry group action consider Example 2.1.

Example 2.1: Note that vertex v_1 and vertex v_2 in Figure 2.2 both have one directed edge to the sink and one directed edge to each other. The symmetry group, in cycle notation, might be represented as $G = \{(v_1v_2), (s)\}$. This partitions the vertices into the orbits $Gv_1 = \{v_1, v_2\}$, $Gs = \{s\}$ so that $V^G = \{Gv_1, Gs\}$.

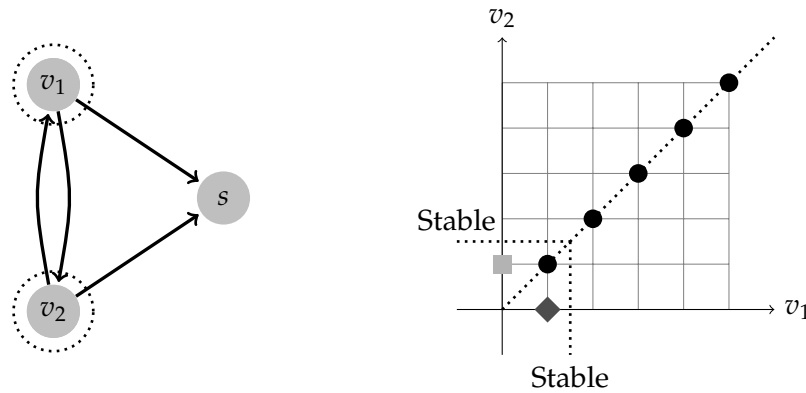


Figure 2.3: The symmetric sandpiles are along the line $v_1 = v_2$. If we start with a sandpile on that line, it will stabilize to a symmetric sandpile.

If both of these vertices had equal amounts of sand, we might consider toppling them in unison. Suppose we have a sandpile $\sigma = (2, 2)$ on the vertices. Subtracting the rows of the reduced Laplacian, the stabilization of this sandpile is given by $\sigma^\circ = \sigma - r_1 - r_2 = (2, 2) - (2, -1) - (-1, 2) = (1, 1)$. Note that we would have achieved the same result if we had subtracted the two rows in unison, that is subtracted the sum of the rows in the symmetric equivalence class.

Sum the rows in each equivalence class:

$$\tilde{\Delta} = \begin{matrix} & v_1 & v_2 \\ v_1 & \begin{pmatrix} 2 & -1 \\ -1 & 2 \end{pmatrix} \\ v_2 & \end{matrix}$$

$$\tilde{\Delta}^G = \begin{matrix} & v_1 & v_2 \\ v_1 + v_2 & \begin{pmatrix} 1 & 1 \\ 1 & 1 \end{pmatrix} \end{matrix} \rightarrow (1)$$

We call this new Laplacian formed by summing rows corresponding to vertices in the same orbit the *symmetrized Laplacian* and denote it $\tilde{\Delta}^G$.

To consider this notion of a symmetrized Laplacian in more detail, we look to the larger Example 2.2.

Example 2.2: In Figure 2.4 we notice that both vertices v_2 and v_5 have all the same properties and structure, and if we were to interchange them, the system represented by our graph would have all the same dynamics.

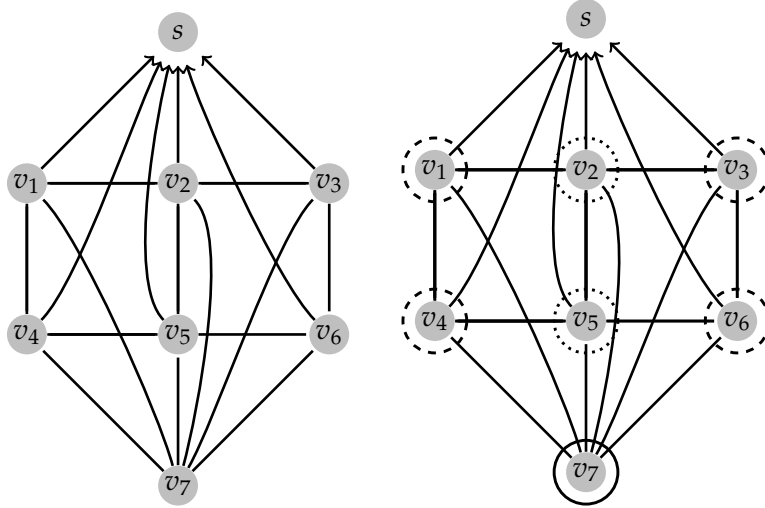


Figure 2.4: Group Action Partitions Vertices into Equivalence Classes.

They belong to the same orbit $Gv_2 = \{v_2, v_5\}$. Likewise the corners, $Gv_1 = \{v_1, v_3, v_4, v_6\}$ and the lone vertex $Gv_7 = \{v_7\}$ all comprise orbits under the symmetries of the graph.

The reduced Laplacian of this graph is given by the matrix:

$$\tilde{\Delta} = \begin{pmatrix} 4 & -1 & 0 & -1 & 0 & 0 & -1 \\ -1 & 5 & -1 & 0 & -1 & 0 & -1 \\ 0 & -1 & 4 & 0 & 0 & -1 & -1 \\ -1 & 0 & 0 & 4 & -1 & 0 & -1 \\ 0 & -1 & 0 & -1 & 5 & -1 & -1 \\ 0 & 0 & -1 & 0 & -1 & 4 & -1 \\ -1 & -1 & -1 & -1 & -1 & -1 & 6 \end{pmatrix}.$$

Now we identify the rows of the reduced Laplacian corresponding to each orbit and we sum them to obtain new “rows.”

Orbits	$(v_1, v_2, v_3, v_4, v_5, v_6, v_7)$
$\{v_1, v_3, v_4, v_6\}$	$(3, -2, 3, 3, -2, 3, -4)$
$\{v_2, v_5\}$	$(-1, 4, -1, -1, 4, -1, -2)$
$\{v_7\}$	$(-1, -1, -1, -1, -1, -1, 6)$

Next we select a representative column from each equivalence class to ob-

tain a new Laplacian matrix:

$$\tilde{\Delta}^G = \begin{pmatrix} 3 & -2 & -4 \\ -1 & 4 & -2 \\ -1 & -1 & 6 \end{pmatrix}.$$

With these examples in mind we can make some more observations about the group action's effect.

2.3 Summary of Notation

In this section we construct a table to keep track of all the algebraic objects we have defined. For examples, we refer exclusively to the graphs in Figures 2.2 and 2.4, denoted $\Gamma_{2.2}$ and $\Gamma_{2.4}$.

- $\Gamma(V, E, s)$: Directed graph with a vertex set, edge set, and global sink.
- $\mathbb{N}^V, \mathbb{Z}^V$: The set of all mappings ϕ that map the vertex set V into the natural numbers or the integers, respectively.
- $\mathbb{Z}V, \mathbb{N}V$: The free abelian group on V , and $\mathbb{N}V \subset \mathbb{Z}V$.
- Δ_Γ : The Laplacian of the graph Γ .
- \tilde{V} : The vertex set minus the sink, $V \setminus s$.
- $\tilde{\Delta}_\Gamma$: The Laplacian of Γ , with the row and column corresponding to the sink deleted.
- $Row(\tilde{\Delta}_\Gamma)$: The image of $\tilde{\Delta}_\Gamma$, or the integer span of its rows.
- $S(\Gamma)$: The sandpile group of Γ , defined by $\mathbb{Z}\tilde{V} / Row(\tilde{\Delta}_\Gamma)$.
- G : The group of symmetries of Γ . (For $\Gamma_{2.2}$, the symmetry group, in cycle notation, consists of $\{(s), (v_1 v_2)\}$.)
- $S(\Gamma)^G$: The *symmetric subgroup* of the sandpile group of Γ . It consists of all sandpiles $\sigma \in S(\Gamma)$ such that $g\sigma = \sigma$ for all $g \in G$.
- $\tilde{\Delta}_\Gamma^G$: The *symmetrized* reduced Laplacian of Γ . Sum the rows in each orbit and choose a representative column.
- V^G : The set of orbits of the vertex set under the symmetry group action G .

2.4 The Symmetric Sandpile Subgroup

We have seen several examples of the behavior of the symmetry group action on the graph $\Gamma(V, E, s)$. Because of the relationship between the vertices of the graph and the sandpiles mapped to them, it is natural to deduce that G induces an action on the sandpile group, $S(\Gamma)$. We present the following explorations from Perkinson (2008b).

Claim 2.1: The action of G commutes with stabilization. That is, if σ is any configuration on Γ , the $g\sigma^\circ = (g\sigma)^\circ$.

Proof. The stabilization of a sandpile σ consists of toppling sand on a sequence of vertices, v_1, \dots, v_n . Then

$$\sigma^\circ = \sigma - \sum_{i=1}^n \tilde{\Delta}^T v_i.$$

At the m -th step in the stabilization process, σ has partially stabilized to the configuration $\sigma' := \sigma - \sum_{i=1}^m \tilde{\Delta}^T v_i$. If a vertex v is unstable in σ' then gv is unstable in $g\sigma' = g\sigma - \sum_{i=1}^m \tilde{\Delta}^T gv_i$. Thus, a sequence of vertices, gv_1, \dots, gv_t can topple, resulting in the stable configuration

$$(g\sigma)^\circ = g\sigma - \sum_{i=1}^t \tilde{\Delta}^T gv_i.$$

□

Corollary 2.1: The action of G preserves recurrent configurations, that is, for each recurrent configuration σ and each $g \in G$, it follows that $g\sigma$ is recurrent.

Proof. Since σ is recurrent, we can find a configuration τ such that $\sigma = (\tau + \sigma_{\max})^\circ$. Then,

$$\begin{aligned} g\sigma &= g(\tau + \sigma_{\max})^\circ \\ &= (g\tau + g\sigma_{\max})^\circ \\ &= (g\tau + \sigma_{\max})^\circ. \end{aligned}$$

Thus, by definition, $g\sigma$ is recurrent. □

Corollary 2.2: If σ is a symmetric configuration, then so is its stabilization, σ° .

Proof. Consider that for all $g \in G$, if $g\sigma = \sigma$, then $g\sigma^\circ = (g\sigma)^\circ$ by Proposition 2.1. \square

Theorem 2.1: *The symmetric, recurrent configurations, $S(\Gamma)^G$, form a subgroup of the sandpile group $S(\Gamma)$.*

Proof. Since the group action respects addition and stabilization in $\mathbb{N}\tilde{V}$, the sum of two symmetric recurrent configurations is again symmetric and recurrent. There is at least one symmetric recurrent configuration, namely, σ_{\max} . This is enough to show that $S(\Gamma)^G$ forms a subgroup of $S(\Gamma)$ since the sandpile group is finite. \square

Chapter 3

Developing a Quotient Graph

Intriguing structure emerges as we allow the symmetry group of a graph to act on its vertices. Section 2.4 outlines some recent theorems related to the symmetric subgroup of a graph's sandpile group. Recall that we are interested in finding a graph that embodies all of the structure of the original graph under the symmetry group action in the hope that it will help us answer questions related to domino tilings as outlined in Section 2.1. Consider the following question.

Question 3.1: Given a graph Γ with symmetric sandpile subgroup $S(\Gamma)^G$, does there exist a quotient graph Γ/G whose sandpile group is isomorphic to the symmetric subgroup of the given graph, $S(\Gamma)^G$?

One logical definition for a quotient graph might be to consider “folding up” the original graph along its symmetries. Consider the vertices to be the orbits of the vertices in the original graph under G , and simply add the

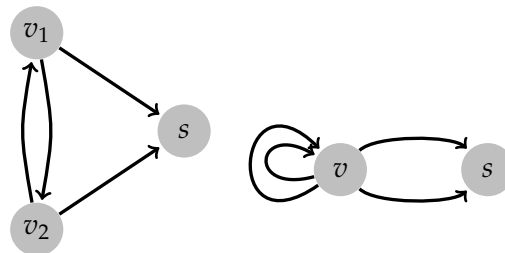


Figure 3.1: “Fold up” the graph along its symmetries to obtain the quotient graph.

weights of edges going from orbit to orbit as depicted in Figure 3.1. More precisely,

Definition 3.1: Given the graph $\Gamma = (V, E, s)$, define the *quotient graph* Γ/G to be a graph with the vertex set V^G , and for each directed edge $(v_i, v_j) \in E$, there is a directed edge, (Gv_i, Gv_j) , in Γ/G such that weight of that edge is given by $\sum_{g \in G} w(gv_i, gv_j)$.

3.1 The Row Quotient

Recall that we defined the symmetrized Laplacian, $\tilde{\Delta}^G$, to be the matrix obtained by summing up the rows corresponding to vertices in the same orbit, and then choosing a representative row. There is a natural isomorphism between the following objects: $\mathbb{Z}\tilde{V}^G / \text{Row}(\tilde{\Delta}^G) \cong (\mathbb{Z}\tilde{V} / \text{Row}(\tilde{\Delta}))^G = S(\Gamma)^G$. That is, the subset of symmetric sandpiles modulo the symmetrized Laplacian is isomorphic to the symmetric sandpile subgroup.

Until now, we have defined the sandpile group $S(\Gamma)$ to be the group quotient $\mathbb{Z}\tilde{V} / \text{Row}(\tilde{\Delta})$. To help simplify notation and allow the following proof to proceed in a more natural way, we define the following groups. Let

- $\tilde{\mathcal{L}}$ be the integer column span of $\tilde{\Delta}^T$ and
- $\tilde{\mathcal{L}}^G$ be the integer column span of $(\tilde{\Delta}^G)^T$,

so, for example, we have $S(\Gamma) = \mathbb{Z}\tilde{V} / \tilde{\mathcal{L}}$.

Theorem 3.1: Recall that $\mathbb{Z}\tilde{V}^G$ is the free abelian group on the set \tilde{V}^G , the set of orbits of the non-sink vertices of Γ under the symmetry group action G . Then $\mathbb{Z}\tilde{V}^G / \tilde{\mathcal{L}}^G \cong (\mathbb{Z}\tilde{V} / \tilde{\mathcal{L}})^G$.

Proof. Consider the mapping $\pi : \mathbb{Z}\tilde{V}^G \rightarrow \mathbb{Z}\tilde{V} / \tilde{\mathcal{L}}$ such that $\sigma \in \mathbb{Z}\tilde{V}^G \subseteq \mathbb{Z}\tilde{V}$ is sent to its equivalence class in $\mathbb{Z}\tilde{V} / \tilde{\mathcal{L}}$. The image of $\sigma \in \tilde{\mathcal{L}}^G$ is 0 since $\tilde{\mathcal{L}}^G \subseteq \tilde{\mathcal{L}}$. This gives the induced mapping:

$$\psi : \mathbb{Z}\tilde{V}^G / \tilde{\mathcal{L}}^G \rightarrow \mathbb{Z}\tilde{V} / \tilde{\mathcal{L}},$$

that maps equivalence classes to equivalence classes in the two quotient groups. We divide the proof into two claims:

Claim 3.1: The image of ψ is equal to the symmetric sandpile subgroup: $\text{Im}(\psi) = S(\Gamma)^G$.

- $Im(\psi) \subseteq S(\Gamma)^G$

Note that this is not immediately clear. We need to show that if an equivalence class in $S(\Gamma)$ contains a symmetric vector, then the (unique) recurrent configuration in that class is also symmetric. Take any symmetric configuration $\tau \geq \sigma_{max}$ with $\tau = 0$ modulo $\tilde{\mathcal{L}}$.

for example, one could take $\tau = |S(\Gamma)|\sigma_{max}$. Let $\sigma \in \mathbb{Z}\tilde{V}$ be a symmetric sandpile configuration. Then so is $\tau + \sigma$ and τ can stabilize by toppling symmetric vertices to see that $(\tau + \sigma)^\circ$, the recurrent element representing σ , is symmetric. Thus, $Im(\psi) \subseteq S(\Gamma)^G$, which proves this claim.

- $Im(\psi) \supseteq S(\Gamma)^G$

This containment is trivial.

Claim 3.2: The kernel of ψ is zero: $ker(\psi) = 0$.

We must show that any symmetric configuration $\sigma \in \tilde{\mathcal{L}}$ is actually an element of $\tilde{\mathcal{L}}^G$. So let $\sigma \in \mathcal{L}$ be symmetric. Say $\sigma = \tilde{\Delta}^T \beta$. Pick any orbit (non-sink) of G , and pick any two vertices in that orbit (note that if the orbit is a fixed point than there is nothing to show).

Let P represent the permutation of the vertices. Thus, thinking of P as a matrix, we have that it is symmetric and idempotent, $P^T = P$ and $P^2 = P$. By the symmetry of Γ , we have that $P\tilde{\Delta}^T = \tilde{\Delta}^T$ and hence $(\tilde{\Delta}^T)^{-1} = P(\tilde{\Delta}^T)^{-1}P$. By symmetry of σ , we have $P\sigma = \sigma$. Now $\beta = (\tilde{\Delta}^T)^{-1}\sigma$ which implies that $P\beta = P(\tilde{\Delta}^T)^{-1}\sigma = [P(\tilde{\Delta}^T)^{-1}P][P\sigma] = (\tilde{\Delta}^T)^{-1}\sigma = \beta$. Thus, β is symmetric, whence $\sigma = \tilde{\Delta}^T \beta \in \tilde{\mathcal{L}}^G$ as required. \square

So we have found an abelian group in terms of the symmetrized Laplacian that is isomorphic to the symmetric subgroup of the graph Γ . Question 3.1 asks for a *graph* whose sandpile group might be this object. The natural graph would come from the symmetrized Laplacian, $\tilde{\Delta}^G$. Recall from Example 2.1 we computed the symmetric sandpile subgroup to be only the sandpile $(1, 1)$. Also we computed the symmetrized Laplacian to be the matrix (1) . Considering the graph with one vertex with one directed edge to the sink, we find the only stable configuration is the zero configuration, (0) . In this simple example, and others, the graph corresponding to the symmetrized Laplacian answers Question 3.1. However, this is not always the case. For the graph in Figure 3.2 recall that the symmetrized

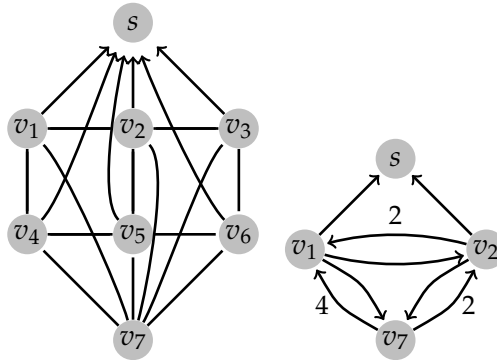


Figure 3.2: The graph on the right is the graph corresponding to the transpose of the symmetrized Laplacian, $(\tilde{\Delta}^G)^T$.

Laplacian was given by the following matrix:

$$\tilde{\Delta}^G = \begin{pmatrix} 3 & -2 & -4 \\ -1 & 4 & -2 \\ -1 & -1 & 6 \end{pmatrix} \quad (\tilde{\Delta}^G)^T = \begin{pmatrix} 3 & -1 & -1 \\ -2 & 4 & -1 \\ -4 & -2 & 6 \end{pmatrix}$$

We note that $\tilde{\Delta}^G$ does not correspond to a legitimate graph because some of its rows sum to less than zero.

3.2 The Row Quotient Transposed

To ameliorate this issue, we take the transpose of the matrix to obtain $(\tilde{\Delta}^G)^T$ and we let Γ_r/G denote the graph it represents (the quotient obtained from the symmetrized Laplacian, obtained by summing up the rows corresponding to vertices in the same orbit). This graph obtained by taking the transpose of the reduced Laplacian works under many circumstances, however, sometimes neither the symmetrized Laplacian nor its graph correspond to a well defined graph. This is often the case when a graph has *selfish vertices*.

Definition 3.2: Given a graph, $\Gamma = (V, E, s)$, we call a vertex $v \in V$ is *selfish*, if its in-degree exceeds its out-degree.

Consider the graph in Figure 3.3. In this example, the vertex v_2 is selfish. It has out-degree 3, but in-degree 4. Note that the vertices v_3 and v_4 are in the same orbit, so we sum the 3rd and 4th rows of the reduced Laplacian to

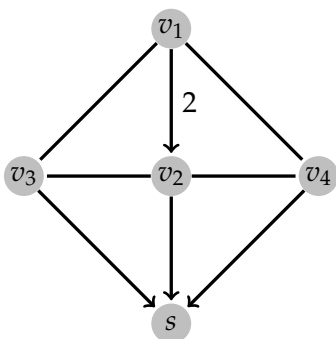


Figure 3.3: The vertex v_2 is selfish: it has in-degree 4, but an out-degree of only 3.

obtain,

$$\tilde{\Delta}^G = \begin{pmatrix} 4 & -2 & -1 \\ 0 & 3 & -1 \\ -2 & -2 & 3 \end{pmatrix} \quad (\tilde{\Delta}^G)^T = \begin{pmatrix} 4 & 0 & -2 \\ -2 & 3 & -2 \\ -1 & -1 & 3 \end{pmatrix}$$

Note that the last row of the symmetrized Laplacian sums to less than zero. The determinant of the symmetrized Laplacian is 18, which is the order of the symmetric subgroup of the graph's sandpile group by Theorem 3.1. Taking the transpose of the symmetrized Laplacian does not help here. The second row sums to less than zero in the transpose. Trying to construct a graph that might correspond to $(\tilde{\Delta}^G)^T$ is futile because we can't have a vertex that has more outgoing edges than its out-degree will allow. Such a graph is not well-defined. This counterexample disqualifies this construction as a good quotient graph in general, though it works in many cases.

3.3 The Column Quotient

Since neither the symmetrized Laplacian nor its transpose always correspond to a well-defined graph, we examine another possible quotient graph. Recall that we require all of the rows of the Laplacian to sum to zero. If we sum the columns of the reduced Laplacian that correspond to vertices in the same orbits, and then choose representative rows, we are always guaranteed a well-defined graph, Γ_c/G . Consider the graph with the selfish vertex whose symmetrized Laplacian failed to produce a legitimate graph in Figure 3.3.

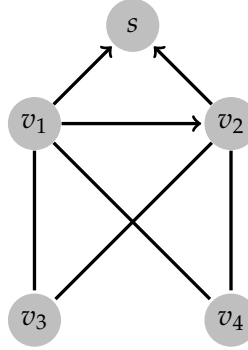


Figure 3.4: The sandpile group for the column quotient graph, $S(\Gamma_c/G) \not\cong S(\Gamma)^G$, for this graph.

$$\tilde{\Delta}_\Gamma = \begin{pmatrix} 4 & -2 & -1 & -1 \\ 0 & 3 & -1 & -1 \\ -1 & -1 & 3 & 0 \\ -1 & -1 & 0 & 3 \end{pmatrix} \quad \tilde{\Delta}_{\Gamma_c/G} = \begin{matrix} & v_1 & v_2 & v_3 + v_4 \\ v_1 & \begin{pmatrix} 4 & -2 & -2 \\ 0 & 3 & -2 \\ -1 & -1 & 3 \end{pmatrix} \end{matrix}$$

Here, using the technique were we sum the columns and then take a representative row, we obtain a Laplacian that does indeed correspond to a legitimate graph, Γ_c/G . The determinate of $\tilde{\Delta}_{\Gamma_c/G}$ is also 18, the same as the determinate of the symmetrize Laplacian. This equality in size is observed every example tried. However, this graph too does not work in general. Consider the following counterexample, the graph given in Figure 3.4. Note that, once again, the vertices v_3 and v_4 are in the same orbit.

$$\tilde{\Delta}_\Gamma = \begin{pmatrix} 4 & -1 & -1 & -1 \\ 0 & 3 & -1 & -1 \\ -1 & -1 & 2 & 0 \\ -1 & -1 & 0 & 2 \end{pmatrix} \quad \tilde{\Delta}_{\Gamma_c/G} = \begin{matrix} & v_1 & v_2 & v_3 + v_4 \\ v_1 & \begin{pmatrix} 4 & -1 & -2 \\ 0 & 3 & -2 \\ -1 & -1 & 2 \end{pmatrix} \end{matrix}$$

Consider also the symmetrized Laplacian,

$$\tilde{\Delta}_\Gamma^G = \begin{matrix} & v_1 & v_2 & v_3, v_4 \\ v_1 & \begin{pmatrix} 4 & -1 & -1 \\ 0 & 3 & -1 \\ -2 & -2 & 2 \end{pmatrix} \end{matrix}$$

We know from Theorem 3.1 that $\mathbb{Z}\tilde{V}^G/\tilde{\Delta}^G \cong S(\Gamma)^G$. Consider the following groups,

$$S(\Gamma)^G = \mathbb{Z}^3 / \left\langle \left(\begin{array}{c} 4 \\ -1 \\ -1 \end{array} \right), \left(\begin{array}{c} 0 \\ 3 \\ -1 \end{array} \right), \left(\begin{array}{c} -2 \\ -2 \\ 2 \end{array} \right) \right\rangle,$$

and,

$$S(\Gamma_c/G) = \mathbb{Z}^3 / \left\langle \left(\begin{array}{c} 4 \\ -1 \\ -2 \end{array} \right), \left(\begin{array}{c} 0 \\ 3 \\ -2 \end{array} \right), \left(\begin{array}{c} -1 \\ -1 \\ 2 \end{array} \right) \right\rangle.$$

We would like to find an isomorphism $\phi : S(\Gamma)^G \rightarrow S(\Gamma_c/G)$. However, consider the Smith normal forms of each of the Laplacians:

$$\begin{aligned} \tilde{\Delta}_{\Gamma_c/G} &= \begin{pmatrix} 4 & -2 & -2 \\ 0 & 3 & -2 \\ -1 & -1 & 3 \end{pmatrix} \rightarrow \begin{pmatrix} 1 & 0 & 0 \\ 0 & 1 & 0 \\ 0 & 0 & 8 \end{pmatrix} \\ &\Rightarrow S(\Gamma_c/G) \cong \mathbb{Z}/8\mathbb{Z}, \end{aligned}$$

however,

$$\begin{aligned} \tilde{\Delta}_{\Gamma}^G &= \begin{pmatrix} 4 & -1 & -1 \\ 0 & 3 & -1 \\ -2 & -2 & 2 \end{pmatrix} \rightarrow \begin{pmatrix} 1 & 0 & 0 \\ 0 & 2 & 0 \\ 0 & 0 & 4 \end{pmatrix} \\ &\Rightarrow S(\Gamma)^G \cong \mathbb{Z}/2\mathbb{Z} \times \mathbb{Z}/4\mathbb{Z}. \end{aligned}$$

Thus there cannot exist an isomorphism, and $S(\Gamma_c/G) \not\cong S(\Gamma)^G$. This conclusion can be confirmed by computing the orders of all the elements in the symmetric sandpile subgroup. None of the symmetric sandpiles have order 8.

3.4 The Folded Quotient

A fourth possibility for a graph that satisfies the desired properties of Γ/G , we might consider a graph whose vertices are the orbits of the vertices of the original graph as before, but this time we take the total sum of the out-degree and the edge weight of all the vertices in the orbit. Any self-loops in the folded quotient graph are simply deleted and not accounted for in the Laplacian. This graph would be similar to the one given by the symmetrized Laplacian, but would generate a much larger sandpile group because the out-degree of its vertices would be much larger.

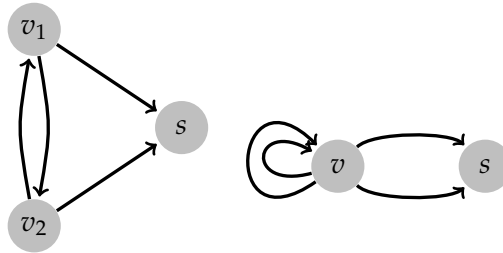


Figure 3.5: For this folded quotient graph, Γ_f/G , we sum the out-degree of all elements of the orbit. Here, $d_{v_1} = d_{v_2} = 2$, this corresponds to the orbit Gv_1 having out-degree $2 + 2 = 4$.

Example 3.1: In this example, we consider the symmetric graph in Figure 3.5. We have previously noted that vertices v_1 and v_2 are in the same orbit under the symmetries of the graph. Consider folding the graph along its symmetries. The reduced Laplacian and accompanying folded quotient Laplacian are given as follows:

$$\tilde{\Delta}_\Gamma = \begin{pmatrix} 2 & -1 \\ -1 & 2 \end{pmatrix} \quad \tilde{\Delta}_{\Gamma_f/G} = v_1 + v_2 \begin{pmatrix} v_1 + v_2 & \\ & 2 \end{pmatrix}$$

Example 3.2: Here we revisit Example 2.2, whose graph appears again in Figure 3.4 along with its folded quotient graph. Consider the dynamics of a vertex in the orbit of v_1 . It has one edge to the sink, one edge to the orbit containing v_7 , one edge to the orbit containing v_2 and finally one edge into its own orbit. We construct a graph in 3.4 that reflects the dynamics of each orbit collectively. Note that any edges between a vertex and another in its own equivalence class is reflected by a self-loop. A sandpile on this new graph seems to correspond to a symmetric sandpile on the original graph. Again, in the folded quotient Laplacian, we simply ignore the self loops. Formally, we define the reduced Laplacian of the folded quotient graph, $\tilde{\Delta}_{\Gamma_f/G}$, to be the matrix obtained by summing both the rows and columns

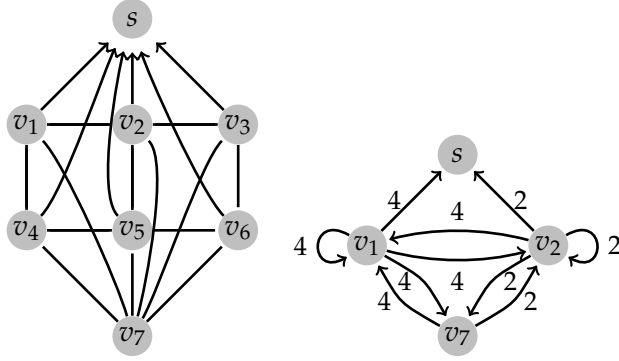


Figure 3.6: An edge between two vertices in the same orbit becomes a self-loop.

of $\tilde{\Delta}_\Gamma$. Consider the folded quotient Laplacian for the graph in Figure 3.4.

$$\tilde{\Delta}_\Gamma = \begin{pmatrix} 4 & -1 & 0 & -1 & 0 & 0 & -1 \\ -1 & 5 & -1 & 0 & -1 & 0 & -1 \\ 0 & -1 & 4 & 0 & 0 & -1 & -1 \\ -1 & 0 & 0 & 4 & -1 & 0 & -1 \\ 0 & -1 & 0 & -1 & 5 & -1 & -1 \\ 0 & 0 & -1 & 0 & -1 & 4 & -1 \\ -1 & -1 & -1 & -1 & -1 & -1 & 6 \end{pmatrix}$$

$$\tilde{\Delta}_{\Gamma_f/G} = \begin{matrix} & Gv_1 & Gv_2 & Gv_7 \\ \begin{matrix} Gv_1 \\ Gv_2 \\ Gv_7 \end{matrix} & \begin{pmatrix} 12 & -4 & -4 \\ -4 & 8 & -2 \\ -4 & -2 & 6 \end{pmatrix} \end{matrix}.$$

Theorem 3.2: *The map $\psi : S(\Gamma)^G \rightarrow S(\Gamma_f/G)$ is injective.*

Proof. Given a graph, $\Gamma(V, E, s)$ with symmetry group G , suppose that there are k orbits in $|\tilde{V}^G|$. We begin by defining a diagonal matrix, $D_{|\tilde{V}^G|}$, with the size of the orbits in \tilde{V}^G along the diagonals.

$$D_{|\tilde{V}^G|} = \begin{pmatrix} |Gv_1| & 0 & \cdots & 0 \\ 0 & |Gv_2| & \cdots & 0 \\ \vdots & & \ddots & \vdots \\ 0 & 0 & \cdots & |Gv_k| \end{pmatrix}.$$

For the folded quotient laplacian in Figure this diagonal matrix is given by,

$$D_{|\tilde{V}^G|} = \begin{pmatrix} 4 & 0 & 0 \\ 0 & 2 & 0 \\ 0 & 0 & 1 \end{pmatrix}.$$

Note that $\tilde{\Delta}^G D_{|\tilde{V}^G|} = \tilde{\Delta}_{\Gamma_f/G}$, by the construction of the folded quotient Laplacian. While a multiplicative inverse of this matrix cannot be defined over the integers, we can create an object defined over the rational numbers,

$$D_{|\tilde{V}^G|}^{-1} = \begin{pmatrix} 1/|Gv_1| & 0 & \cdots & 0 \\ 0 & 1/|Gv_2| & \cdots & 0 \\ \vdots & & \ddots & \vdots \\ 0 & 0 & \cdots & 1/|Gv_k| \end{pmatrix}.$$

Note that the diagonal entries of this “inverse” will never be undefined, because there will always be at least one element in each orbit. Given this definition, we can write $\tilde{\Delta}^G = \tilde{\Delta}_{\Gamma_f/G} D_{|\tilde{V}^G|}^{-1}$, which will yield a matrix over the integers by the construction of $\tilde{\Delta}_{\Gamma_f/G}$.

Define the mapping

$$\begin{aligned} \pi &: \mathbb{Z}\tilde{V} \rightarrow \mathbb{Z}\tilde{V}/\text{Row}(\tilde{\Delta}_{\Gamma_f/G}), \\ \pi &: \sigma \mapsto \sigma D_{|\tilde{V}^G|}, \end{aligned}$$

and consider that its kernel is given by

$$\ker(\pi) = \{\sigma \in \mathbb{Z}\tilde{V} : \pi(\sigma) \in \text{Row}(\tilde{\Delta}_{\Gamma_f/G})\}.$$

This gives the induced mapping $\psi : \mathbb{Z}\tilde{V}/\tilde{\Delta}^G \rightarrow \mathbb{Z}\tilde{V}/\tilde{\Delta}_{\Gamma_f/G}$. To show that ψ is an injection we must show that for $\sigma \in \mathbb{Z}\tilde{V}$, the kernel of the projection mapping is exactly the row span of the symmetrized Laplacian, that is, $\sigma \in \ker(\pi)$ if and only if $\sigma \in \text{Row}(\tilde{\Delta}^G)$. Consider that for all $\sigma \in \mathbb{Z}\tilde{V}$, there exists a $\tau \in \mathbb{Z}\tilde{V}$ such that,

$$\begin{aligned} &\sigma D_{|\tilde{V}^G|} = \tau \tilde{\Delta}_{\Gamma_f/G}, \\ \text{if and only if,} &\quad \sigma = \tau \tilde{\Delta}_{\Gamma_f/G} D_{|\tilde{V}^G|}^{-1} \\ \text{if and only if,} &\quad \sigma = \tau \tilde{\Delta}^G. \quad \square \end{aligned}$$

We have discussed four possible definitions of a quotient graph Γ/G . None of them work in general, though all work for certain types of graphs.

The Sandpile group objects for each of the quotient graphs of the running example graph, depicted originally in Figure 1.3, are listed below. Note that $S(\Gamma_r/G)$ and $S(\Gamma_c/G)$ have the same size as the symmetric sandpile subgroup, $S(\Gamma)^G$, while $S(\Gamma_f/G)$ is larger.

- $S(\Gamma): \{\{1,1\}, \{1,0\}, \{0,1\}\}$
- $S(\Gamma)^G: \{\{1,1\}\}$
- $S(\Gamma_r/G): \{\{0,0\}\}$
- $S(\Gamma_c/G): \{\{0,0\}\}$
- $S(\Gamma_f/G): \{\{1,1\}, \{0,0\}\}$

Does a quotient graph Γ/G exist for a general graph?

Chapter 4

Conclusions and Future Study

The abelian sandpile model describes many different physical phenomena and proves to be related to computer science, combinatorics and theoretical physics. Here we have provided a thorough introduction to the structure and abelian property of the model. In Section 1.5, we have outlined some possible new and simplistic approaches to the standard sandpile theory.

We introduced the notion of a symmetric sandpile on a graph, and showed the set of such sandpiles forms a subgroup of the sandpile group. In addition, we presented several recent theorems related to the special properties of symmetric graphs.

For a given graph Γ with symmetric sandpile subgroup $S(\Gamma)^G$, we defined the quotient graph to be the graph Γ/G whose sandpile group is isomorphic to $S(\Gamma)^G$. The question of the existence of such a quotient graph for general directed graphs remains open. We have introduced two candidates for this quotient graph and shown them to satisfy the desired definition in many cases. The answer to this question may have exciting applications to counting the number of domino tilings of the $2n \times 2n$ grid.

Bibliography

- Bak, Per. 1996. *How Nature Works: The Science of Self-Organized Criticality*. New York: New York: Copernicus.
- Bak, Per, Chao Tang, and Kurt Wiesenfeld. 1987. Self-organized criticality: An explanation of $1/f$ noise. *Physical Review Letters* 59(4):381–384.
- Baker, Matthew. 2007. Specialization of linear systems from curves to graphs. ArXiv:math/0701075v4.
- Behzad, Mehdi, Gary Chartrand, and Linda Lesniak-Foster. 1979. *Graphs and Digraphs*. Belmont: Wadsworth, Inc.
- Cori, Robert, Dominique Rossin, and Bruno Salvy. 2002. Polynomial ideals for sandpiles and their groebner bases. *Theoretical Computer Science* 276(1):1–15.
- Dhar, Deepak. 1990. Self-organized criticality of sandpile automaton models. *Physical Review Letters* 64(14):1613–1616.
- . 1998. The abelian sandpile and related models. *Physica A* 263:4–25.
- . 1999. Studying self-organized criticality with exactly solved models. ArXiv:cond-mat/9909009 v1.
- . 2006. Theoretical studies of self-organized criticality. *Physica A* 369:29–70.
- Holroyd, Alexander E., Linonel Levine, Karola Mészáros, Yuval Peres, James Propp, and David B. Wilson. 2008. Chip-firing and rotor-routing on directed graphs. ArXiv:0801.3306v3.
- Kenyon, Richard W., James G. Propp, and David B. Wilson. 2000. Trees and matchings. *Electronic Journal of Combinatorics* 7:(electronic).

- Merino, Criel. 2005. The chip-firing game. *Discrete Mathematics* 302(1-3):188–210.
- Morar, Daniela, and David Perkinson. 2007. The canonical sandpile on a 2×2 grid. Unpublished Research Report.
- Pachter, Lior. 1997. Combinatorial approaches and conjectures for 2-divisibility problems concerning domino tilings of polyominoes. *Electronic Journal of Combinatorics* 4(R29):electronic.
- Perkinson, David. 2008a. All 2's theorem.
- . 2008b. Lecture notes: Math 412.
- . 2008-2009. Private correspondence.
- Speer, Eugene R. 1993. Asymmetric abelian sandpile models. *Journal of Statistical Physics* 71(1-2):61–74.